Autonomous and 3D real-time multi-beam manipulation in a microfluidic environment

Perch-Nielsen, Ivan R.; Rodrigo, Peter John; Alonzo, Carlo Amadeo; Glückstad, Jesper

Published in:
Optics Express

Link to article, DOI:
10.1364/OE.14.012199

Publication date:
2006

Document Version
Publisher's PDF, also known as Version of record

Autonomous and 3D real-time multi-beam manipulation in a microfluidic environment

Ivan R. Perch-Nielsen, Peter John Rodrigo, Carlo Amadeo Alonzo and Jesper Glückstad

Optics and Plasma Research Department, Risø National Laboratory, DK-4000 Roskilde, Denmark
http://www.ppo.dk
jesper.gluckstad@risoe.dk

Abstract: The Generalized Phase Contrast (GPC) method of optical 3D manipulation has previously been used for controlled spatial manipulation of live biological specimen in real-time. These biological experiments were carried out over a time-span of several hours while an operator intermittently optimized the optical system. Here we present GPC-based optical micromanipulation in a microfluidic system where trapping experiments are computer-automated and thereby capable of running with only limited supervision. The system is able to dynamically detect living yeast cells using a computer-interfaced CCD camera, and respond to this by instantly creating traps at positions of the spotted cells streaming at flow velocities that would be difficult for a human operator to handle. With the added ability to control flow rates, experiments were also carried out to confirm the theoretically predicted axially dependent lateral stiffness of GPC-based optical traps.

OCIS codes: (170.4520) Optical confinement and manipulation, (140.7010) Trapping, (120.1880) Detection, (999.9999) Microfluidics.

References and links

1. A. Ashkin, J. M. Dziedzic, J. E. Bjorkholm, and S. Chu, "Observation of a single-beam gradient force optical trap for dielectric particles," Opt. Lett. **11,** 288–290 (1986).
2. K. Sasaki, M. Koshio, H. Misawa, N. Kitamura, and H. Masuhara, "Pattern formation and flow control of fine particles by laser-scanning micromanipulation," Opt. Lett. **16**, 1463–1465 (1991).
3. D. G. Grier, "A revolution in optical manipulation," Nature **424**, 810-816 (2003).
4. K. Dholakia and P. Reece, "Optical micromanipulation takes hold," Nano Today **1**, 18-27 (2006).
5. J. Glückstad, "Sorting particles with light," Nat. Mater. **3**, 9-10 (2004).
6. A. Terray, J. Oakey, and D. W. M. Marr, "Microfluidic control using colloidal devices," Science **296**, 1841 (2002).
7. L. Kelemen, S. Valkai, and P. Ormos, "Integrated optical motor," Appl. Opt. **45**, 2777-2780 (2006).
8. J. Enger, M. Goksör, K. Ramser, P. Hagberg, and D. Hanstorp, "Optical tweezers applied to a microfluidic system," Lab Chip **4**, 196-200 (2004).
9. J. Glückstad and P. C. Mogensen, "Optimal phase contrast in common-path interferometry," Appl. Opt. **40**, 268-282 (2001).
10. P. J. Rodrigo, V. R. Daria, and J. Glückstad, "Four-dimensional optical manipulation of colloidal particles," Appl. Phys. Lett. **86**, 074103 (2005).
11. N. Arneborg, H. Siegumfeldt, G. H. Andersen, P. Nissen, V. R. Daria, P. J. Rodrigo, and J. Glückstad "Interactive optical trapping shows that confinement is a determinant of growth in a mixed yeast culture," FEMS Microbiol. Lett. **245**, 155-159 (2005).
12. P. J. Rodrigo, L. Gammelgaard, P. Bøggild, I. R. Perch-Nielsen, and J. Glückstad, "Actuation of microfabricated tools using multiple GPC-based counterpropagating-beam traps," Opt. Express **13**, 6899-6904 (2005).
13. I. R. Perch-Nielsen, P. J. Rodrigo, and J. Glückstad, "Real-time interactive 3D manipulation of particles viewed in two orthogonal observation planes," Opt. Express **18**, 2852-2857 (2005).
14. P. J. Rodrigo, I. R. Perch-Nielsen, and J. Glückstad, "Three-dimensional forces in GPC-based counterpropagating-beam traps," Opt. Express **14**, 5812-5822 (2006).

#76472 - $15.00 USD Received 27 October 2006; revised 29 November 2006; accepted 30 November 2006

1. Introduction

Over the past decades, the use of optical forces has proven efficient and versatile for manipulating the motion of mesoscopic objects in a non-invasive manner. Until just a few years ago virtually all optical manipulation schemes were based on the principle of trapping particles inside a single strongly focused beam and subsequent movement to a desired position by translating the laser focus [1, 2].

Within the last few years, it has been realized that much more versatile and general manipulation of particles and cell colonies is possible by using specially tailored structures of light. Such light patterns have unprecedented potential for manipulating mesoscopic objects and have already been successfully used to organize small particles, including microorganisms, in desired patterns and to sort samples of particles according to their size to mention but a few applications [3-5].

Simultaneously, the rapid development of microfluidic technologies have opened a new world of possibilities for the bio/chemical community. Earlier demonstrations of laser assisted microfluidic systems have shown exciting degrees of experimental freedom e.g. the ability to create an arbitrary environment for one or more selected cells, or even the simulation of *in vivo* conditions [6-8].

To fully integrate these unique technology platforms into a next generation of fully parallel and real-time controlled micro- or optofluidic systems, it is desirable to look for ways of automatizing the processes and to ultimately break free from the inherently slow and serial nature of human interfacing and control.

The Generalized Phase Contrast (GPC) method [9] has previously been demonstrating the potential to do exactly this, by supporting *true* real-time and parallel manipulation of a plurality of particles in a 3D environment [10]. In particular, GPC has been applied for performing pioneering yeast cell micro-colony experiments [11]. However, until now all these multi-particle demonstrations have been relying on human supervision at zero or very low flow rates. Here, we demonstrate for the first time an autonomous computerized system that works in parallel within a rapidly changing micro-environment, where cells and suspension media are continuously replenished at high flow rates.

2. Experimental setup

2.1 Optical system

We start by demonstrating the key advantages of combining the GPC approach for optical trapping with a microfluidic system through two simple applications. First, we show how the microfluidic system can assist in the optimization and calibration of the optical trapping system, *i.e.* trap stiffness and other dynamic characteristics can be readily verified. Next, we demonstrate the simplicity by which our automated real-time trapping system can assist in the handling of a microbiological experiment, particularly when the amount of cells carried by the continuous flow might be overwhelming for a human operator.

The GPC-based trapping system achieves particle trapping in the *xy* (transverse) plane due to gradient forces and *z* (axial) trapping due to equilibrium between the scattering forces caused by a set of counterpropagating beams. The optical system, described in detail elsewhere [12, 13], shapes a laser beam into desired intensity distributions with high optical throughput. The real-time synthesized beamlets are subsequently projected into the sample volume using a counter-propagating beam geometry (Fig. 1). Two Olympus LMPL 50xIR objectives provide long working distances, 6.0 mm from each barrel tip, and NA = 0.55. A LabVIEW program handles the spatial light modulators and interfaces with the CCD camera (JAI CV-M4+CL monochrome camera with 2/3" sensor) using LabVIEW standard image acquisition (IMAQ) modules.

#76472 - $15.00 USD Received 27 October 2006; revised 29 November 2006; accepted 30 November 2006

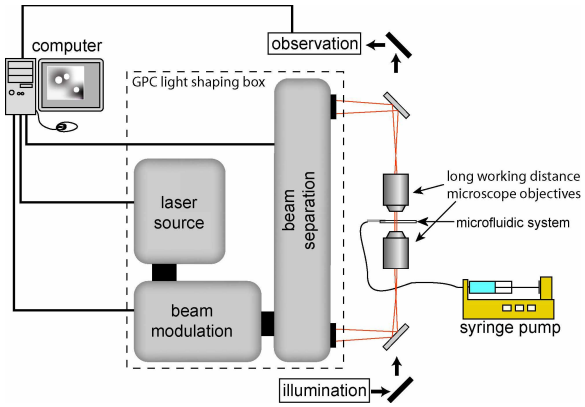

Fig. 1. Schematic diagram of the experimental setup. The long working distance between the objective lenses significantly eases the insertion of a microfluidic system. The computer undertakes multiple tasks such as receiving feedback from an observation module, processing the acquired data and lastly generating control signals used for addressing the spatial light modulation module.

2.2 Microfluidic system

The microfluidic system is a rectangular channel made by stacking microscope glass cover slips of different dimensions, but each with same thickness of ~170 µm. These are assembled using Norland UV adhesive. A 60 mm x 24 mm piece is used as a base and two pieces of 24 mm x 10 mm, slightly displaced with respect to each other, serve as channel walls. One 24 mm x 4 mm piece is positioned to create two inlets into the channel (see Fig. 2). Finally, a cover slip is placed as a lid, and two clinical needles are shaped and glued into position to serve as interface between the channel and the feeding tubes.

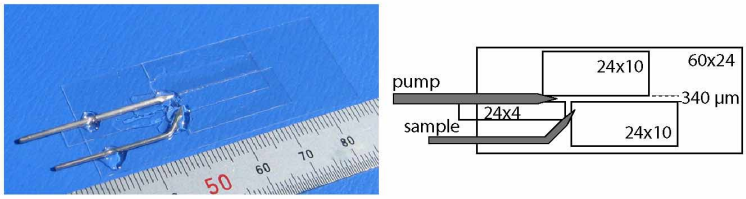

Fig. 2. An image of one of the microfluidic systems and the schematic of the component needles and microscope cover slips.

The functional part of the glass channel (not covered by UV adhesive and accessible by the microscope) has an inner height of 170 µm, a width of 340 µm and a length of 15 mm. The width is achieved by using two cover slips as spacers; it is chosen to reduce the ratio between pump rate and resulting flow velocity and thereby maximizing the range of experimental pump rates.

The needle attaching the tube to the pump have an external diameter of 0.8 mm to secure a short piece of silicon tube with an inner diameter of 0.5 mm, however the needle used for sample inlet is chosen to be 0.6 mm to ease the insertion/removal of a small disposable syringe used for the sample injection.

A 15 cm piece of PTFE tube (inner diameter 0.25 mm) connects the microfluidic system to the syringe pump (Harvard model 11 plus). A selection of glass syringes (Hamilton) ranging from 25 µl to 1 ml is utilized to optimize the pump stroke and for achieving the desired flow rates.

#76472 - $15.00 USD Received 27 October 2006; revised 29 November 2006; accepted 30 November 2006

2.3 Sample preparation

Yeast cells, *Saccharomyces cerevisiae*, are diluted in purified water to cell densities of approximately 1 to 50 cells per 100 µm x 100 µm area within the trapping region. The fluidic system (feeding tube and microsystem) is primed with purified water and air is fully removed. A glass syringe (typically 25 µl) is then attached and the pump is started at a rate in the order of 10 µl/hour. With the channel filled, minor alignment corrections are applied to the optical system to compensate for variations between the different microfluidic systems – this includes fine adjustments in the computer program that ensure proper correlation between the pixels on the spatial light modulator and those on the CCD camera. The sample is then injected through the second channel, which is sufficiently long to keep any incidental air bubbles away from the flow.

3. Experiments and discussion

Due to the parabolic flow profile in a laminar flow at very low Reynolds number, particle velocity will vary depending on the particle's distance from a surface. A flow of 10 µl/hour yields an average flow velocity in the channel (170 µm x 340 µm cross section) of ~50 µm/s. The corresponding peak velocity in the center of the channel is ~75 µm/s. However, due to gravity, particles tend to settle on and creep along the channel floor at a slower rate. Variations in particle velocity along the vertical profile of the structure are avoided by first collecting particles at the (axial) bottom and (lateral) center of the channel. The flow rate (µl/hour) is then calibrated to particle speed (µm/s) for a given microstructure by measuring particle displacement for a given time for different flow rates (usually 10 to 100 µl/hour).

3.1 Particle lift and escape

To illustrate the trapping properties of the light beams used in the GPC-setup, the top beam was disabled such that particles were lifted upwards from the bottom as illustrated in Fig. 3. This reduces the total trapping power compared to having both beams on, but enables us to evaluate the *z*-dependency of the trap stiffness. At some point, as the beam elevates a particle from the channel floor into a region with higher fluid velocity, the increasing force exerted by the fluid exceeds the strength of the optical trap and the cell is carried downstream (see Fig. 3 right). Escape velocities of yeast cells were observed to be cell size dependent and measured to lie between 60 to 80 µm/s using a single beam trap (diameter at focal point: 5 µm, measured power: 10 mW).

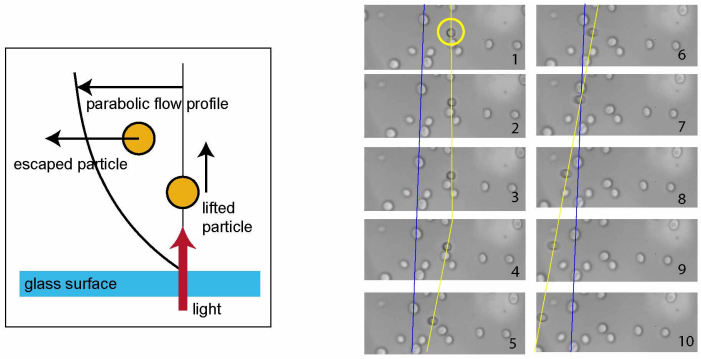

Fig. 3. Left: Illustrating the particle dynamics in a lift and escape experiment. Forward movement is temporarily stopped while the optical trap lifts the particle. Right: Sequence of images showing yeast cells in a flow, 200 ms between successive frames. The yellow line represents the position of the trapped cell, which exits the trap between frame 3 and 4, the dark blue line indicates a free flowing cell. The exit velocity of the optically lifted yeast cell is greater than 60 µm/s, approximately 6 times that of a free flowing cell.

Escape velocity is a function of two opposing factors: trap strength and fluid velocity. In a simple model that approximates each optical trap as a collimated "column of light" through

#76472 - $15.00 USD Received 27 October 2006; revised 29 November 2006; accepted 30 November 2006

the trapping volume, the lateral trap strength is uniform along the axial direction. The measured lateral escape velocity should then be independent of the bulk flow rate. The particle would break free of the trap as soon as it reaches an axial position where the local fluid velocity exceeds the fixed trap strength. However, considering the more detailed model of light propagation for GPC-generated traps discussed in Ref. [14], trapping strength is expected to vary with particle position along the beam propagation direction. Increasing the bulk flow rate alters the fluid velocity profile thus changing the critical position at which fluid velocity exceeds the axially varying trap strength. Such variation is observed in Fig. 4.

3.2 Three-dimensional manipulation in a flow

Yeast cells were lifted above the bottom surface by the optical traps and moved around independently while retaining a flow of the fluid surrounding the cells. Due to the parabolic flow profile upwards through the channel, the surrounding fluid velocity would move the cells at different positions with velocities ranging from 10 to more than 60 μm/s.

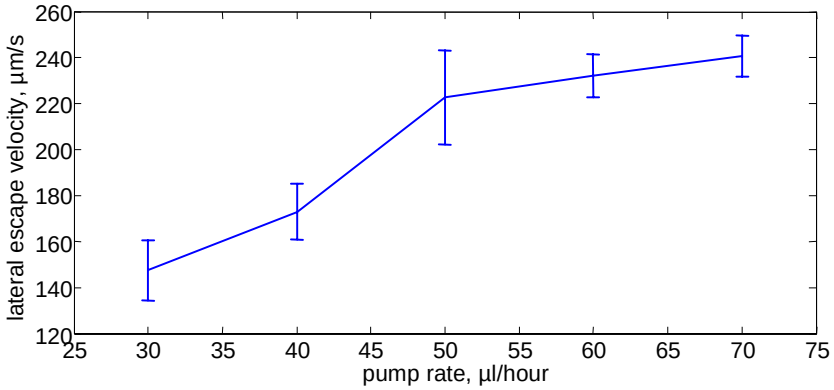

Fig. 4. Mean values of escape velocities of 6 μm polystyrene beads as a function of pump rate. Particle size 5.68 μm. 50-100 data points per pump rate. Error bars are the std. deviation; the main contribution is pulsation of the syringe pump. Microbead escape velocity is significantly larger than measured for the yeast cells, due to the smaller size and higher refractive index of the polystyrene beads compared to that of the cell.

Real-time, interactive optical manipulation of multiple living yeast cells in 3D within the microfluidic system is shown in Fig. 5. The trapped cells are kept in a group close together to minimize the risk of collision with incoming cells. Due to limitations inherited from a serial computer mouse interface, a human operator can easily be overwhelmed by incoming cells carried through the trapping volume by the fluid.

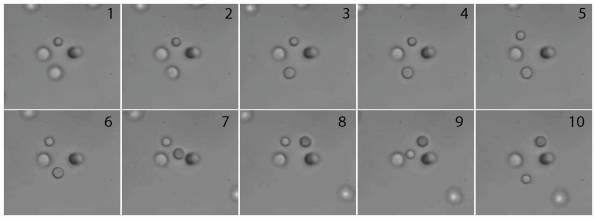

Fig. 5. Realtime interactive manipulation of yeast cells in a microfluidic system (0.75 s between frames). Free moving cells are out of focus and creeping from left to right along the lower surface at ~10 μm/s. Five yeast cells are trapped (rightmost trap contains two cells). The yeast cells that are lifted into focus enter a region with flow velocity exceeding 50 μm/s (estimated by turning off traps). Frames 1-3: the lower cell is lifted. Frames 4-10: the upper and lower cells are repositioned by the user via computer mouse control.

#76472 - $15.00 USD Received 27 October 2006; revised 29 November 2006; accepted 30 November 2006

3.3 Cell detection and locking

A major advantage of GPC-based optical manipulation is that no computation is required to calculate the desired trapping pattern. There is a direct mapping from the SLM pattern to the light intensity distribution in the sample volume. We capitalize on the ease and speed by which trapping patterns can be manipulated by introducing an automation extension to the LabVIEW control program. Since the extension interfaces directly with the fully interactive main program, the user has – at any time – full control to move, add and remove traps in co-operation with the extension. It would however be a stressful task, since the time available to react is low due to the amount of cells arriving with the flow, combined with the fact that only a single trap (or one group of traps) at a time can be moved using the mouse controlled interface.

A detection area is defined in the image together with a set of detection parameters (e.g. minimum and maximum size of incoming cells) for identifying targets to trap. The core of the detection and trapping subroutine consists of 6 steps: 1. Obtain video image from camera. 2. Detect cells. 3. Discard those already having a trap. 4. Set trap at cell position. 5. Save image file for reference. 6. If more than N cells are trapped, discard traps and wait.

The automated system demonstrated the capability to detect and capture cells with high efficiency, even at cell concentrations and flow rates that might overwhelm a human operator. When the detection algorithm is enabled, it freezes all detected cells in the designated area, however further incoming cells tend to stack at the upstream edge of the detection area. The performance of the system appears to be limited only by the bunching of passing particles.

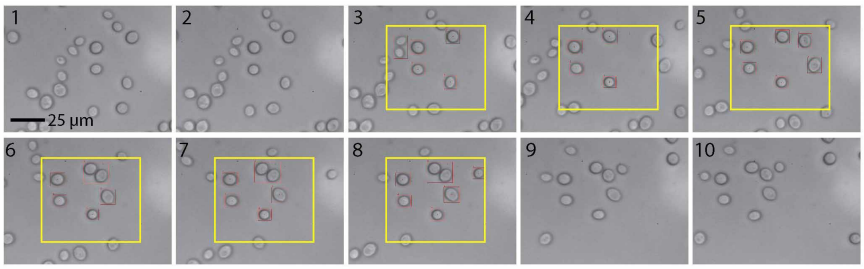

Fig. 6. (AVI: 2.5 MB) Detection and trapping of cells (0.75 s between successive frames). The square marks the detection/trapping area. When the square is off, the cells are released. The flow is set to 20 µl/hour, giving a cell velocity of approximately 15 µm/s. Note the two cells top-left in the detection area of frame 3; they are close together and both relatively small and therefore detected as one cell, resulting in the creation of a single common trap.

The program can easily be extended to provide further functionality in handling the trapped cells, *e.g.* lifting them from the floor into the faster flow stream. Further automated image analysis could also be carried out on trapped cells, such as measuring cell size or the circularity of the cell as an indication of cell growth. Automated software macros for doing simple tasks are also possible. For example, when several particles are collected in one trap they tend to stack up. It is possible to single them out in individual traps by oscillating the trap rapidly. The computer is capable of performing such a task faster and more reliably than shaking the trap by hand using a computer mouse.

4. Conclusion

We have successfully integrated a microfluidic system with a GPC-based optical trapping workstation. This enabled us to demonstrate the first autonomous and 3D real-time multi-cell laser-manipulation in a microfluidic environment. Measurements assessing the axial stiffness of GPC-based beam traps indicated an axial dependence as theoretically predicted [14]. Furthermore, we found that the operator can be aided in the detection of cells. Even with just the modest processing power of a standard desktop computer, the system is capable of detecting and locking onto cells at a much faster rate than possible for a human operator alone. Thus, the operator can be relieved of doing tedious or time-consuming tasks. The cells

#76472 - $15.00 USD Received 27 October 2006; revised 29 November 2006; accepted 30 November 2006

can be maintained at a given position after trapping until a more elaborate experiment can take place. With the aid of a microfluidic system, this can involve the replacement of the sample fluid with one carrying growth media or other chemical substances that imitate special environments for microbiological experiments.

5. Acknowledgment

We would like to thank the support from the EU-FP6-NEST program (ATOM3D), the ESF-Eurocores-SONS program (SPANAS) and the Danish Technical Scientific Research Council (FTP).

#76472 - $15.00 USD Received 27 October 2006; revised 29 November 2006; accepted 30 November 2006